

# Polycationic disorder in $[\text{Bi}_6\text{O}_4(\text{OH})_4](\text{NO}_3)_6$ : Structure determination using synchrotron radiation and microcrystal X-ray diffraction

N. Henry<sup>a,\*</sup>, O. Mentré<sup>a</sup>, F. Abraham<sup>a</sup>, E.J. MacLean<sup>b</sup>, P. Roussel<sup>a</sup>

<sup>a</sup>UCCS, Equipe de Chimie du Solide, UMR CNRS 8181, ENSC Lille–UST Lille, BP 90108, 59652 Villeneuve d'Ascq Cedex, France

<sup>b</sup>CCLRC Daresbury Laboratory, Warrington WA4 4AD, Cheshire, UK

Received 23 February 2006; received in revised form 14 April 2006; accepted 29 May 2006

Available online 13 June 2006

## Abstract

The bismuth basic nitrate  $[\text{Bi}_6\text{O}_4(\text{OH})_4](\text{NO}_3)_6$  crystallizes in a rhombohedral hexagonal unit cell with parameters  $a = 15.1332(6) \text{ \AA}$ ,  $c = 15.7909(9) \text{ \AA}$ ,  $V = 3131.8(3) \text{ \AA}^3$ ,  $Z = 6$ , space group  $R\bar{3}$ . The synthesis, formula determination, thermogravimetric analysis and nitrate assay, and finally, its crystal structure refinement determined at 150(2) K by synchrotron X-ray microcrystal diffraction are reported. Its structure is built from  $[\text{Bi}_6\text{O}_4(\text{OH})_4]^{6+}$  polycations, six per unit cell, disordered over two positions. Two oxygen atoms are common to the two antagonist polycations (full occupancy) while the remaining six are partially occupied. The  $[\text{Bi}_6\text{O}_4(\text{OH})_4]^{6+}$  hexanuclear clusters form columns along the  $c$ -axis. The cohesion between polycationic entities is effected by nitrate anions through either OH–ONO<sub>2</sub> hydrogen bonds or Bi–ONO<sub>2</sub> bonds. One of the two independent  $[\text{NO}_3]^-$  groups is also disordered over two positions. Only a local order in the columns is obtained by formation of pairs of ordered  $[\text{Bi}_6\text{O}_4(\text{OH})_4]^{6+}$  polycations.

© 2006 Elsevier Inc. All rights reserved.

**Keywords:** Anhydrous bismuth basic nitrate; Synchrotron X-ray; Microcrystal diffraction; Structure determination

## 1. Introduction

About 15 bismuth basic nitrates have already been reported in the literature since the 17th century [1]. There is some confusion in the old literature about the existence and formation of these compounds mainly due to the great variety of compounds and to the difficulties encountered in their chemical analyses, crystal growth and in preparation of pure phases. Other crystallographic reasons are based on the quasi-systematic existence of twins and/or superstructure, and the great contrast in the X-ray scattering factor between heavy bismuth and lighter oxygen or nitrogen atoms. In fact, only few compounds have been unequivocally confirmed by recent structural investigations. The bismuth basic nitrates have preliminarily been studied for their medical applications [2]. They are also interesting as a precursor for bismuth oxide in soft

chemistry [3]. Up to now, four compounds showing similar  $[\text{Bi}_6\text{O}_x(\text{OH})_{8-x}]^{(10-x)+}$  polycations have been structurally characterized:  $[\text{Bi}_6\text{O}_5(\text{OH})_3](\text{NO}_3)_5 \cdot 3\text{H}_2\text{O}$  [4],  $[\text{Bi}_6\text{O}_4(\text{OH})_4](\text{NO}_3)_6 \cdot 4\text{H}_2\text{O}$  [5],  $[\text{Bi}_6\text{O}_4(\text{OH})_4](\text{NO}_3)_6 \cdot \text{H}_2\text{O}$  [6] and  $[\text{Bi}_6\text{O}_{4.5}(\text{OH})_{3.5}]_2(\text{NO}_3)_{11}$  [7]. As an illustration of the confusing interpretation enounced above, the title compound has been first assigned to  $\text{Bi}(\text{NO}_3)\text{O} \cdot \text{H}_2\text{O}$  with  $a = 15.57 \text{ \AA}$  and  $c = 7.6 \text{ \AA}$  [8–10] and more recently to  $[\text{Bi}_6\text{O}_5(\text{OH})_3](\text{NO}_3)_5 \cdot 2\text{H}_2\text{O}$  with  $a = 15.185(1) \text{ \AA}$  and  $c = 15.834(2) \text{ \AA}$  [11]. We will see, in the present report that the first errors on the  $c$  parameter can be assigned to the presence of a superstructure with  $c \times 2$ . The presence of loosely bound water molecules or hydroxyl groups, e.g. O versus OH in  $[\text{Bi}_6\text{O}_x(\text{OH})_{8-x}]^{(10-x)+}$  polycations, complicates the formula determination. It is then generally completed by spectroscopic analysis but still may lead to formula errors. We report herein the synthesis, the formula determination and the structure determination from microcrystals of  $[\text{Bi}_6\text{O}_4(\text{OH})_4](\text{NO}_3)_6$ , with disordered  $[\text{Bi}_6\text{O}_x(\text{OH})_{8-x}]^{(10-x)+}$  polycations.

\*Corresponding author. Fax: +33 3 20 33 68 14.

E-mail address: [natacha.henry@ensc-lille.fr](mailto:natacha.henry@ensc-lille.fr) (N. Henry).

## 2. Experimental

### 2.1. Powder synthesis

$\text{Bi}_2\text{O}_3$ , 0.5 g, (Aldrich, 99.99%) was dissolved in a 2 mL nitric acid solution (70%, sds). This solution was added drop wise to 200 mL of a 50/50 water/ethanol solution. The precipitate was filtered, washed with water and dried at room temperature. A white powder was obtained containing crystals, which were too small for conventional laboratory X-ray single crystal experiments (typical crystal dimensions ca.  $\sim 0.045 \times 0.005 \times 0.005 \text{ nm}^3$ ). All attempts to grow larger crystals using different solvents, temperatures or synthesis methods were unsuccessful.

### 2.2. Formula determination

Prior to the single crystal experiments, several investigations were carried out to obtain the main details about the title compound formulation.

#### 2.2.1. Powder diffraction data indexing

Powder diffraction data were collected with a D5000 Siemens diffractometer in a Bragg–Brentano setup. The powder pattern was indexed using the TREOR program [12], giving a rhombohedral hexagonal unit cell with parameters  $a = 15.1332(6) \text{ \AA}$  and  $c = 15.7909(9) \text{ \AA}$ ; this corresponds to the previously reported lattice parameters for the erroneously announced  $[\text{Bi}_6\text{O}_5(\text{OH})_3](\text{NO}_3)_5 \cdot 2\text{H}_2\text{O}$  formulation [11].

#### 2.2.2. Thermogravimetric analysis

The molar weight has been obtained by thermogravimetric analysis (TGA) coupled with differential thermal analysis, collected on a TGA 92 SETARAM apparatus. Experiments were undertaken in air with a  $5^\circ\text{C min}^{-1}$  heating rate between room temperature and  $630^\circ\text{C}$  (Fig. 1). The total weight loss of 20.7%, and the identification by XRD of  $\alpha\text{-Bi}_2\text{O}_3$  as the decomposition product, led to a molar weight of  $293.1 \text{ g mol}^{-1}$  with one Bi atom per formula unit. Using high-temperature XRD (Guinier–Lenné–  $20\text{--}700^\circ\text{C}$  in 60 h), it was possible to identify the intermediate formation, at  $530^\circ\text{C}$ , of  $\text{Bi}_5\text{O}_7\text{NO}_3$  [13], which agrees perfectly with the weight loss (4.4%) observed

between  $530$  and  $630^\circ\text{C}$  ( $\text{Bi}_5\text{O}_7\text{NO}_3 \rightarrow 5/2 \text{ Bi}_2\text{O}_3 + 1 \text{ NO} + 3/4 \text{ O}_2$ ). Using these results and the value of the observed density measured with a helium Micromeritics (AccuPyc 1330) pycnometer, ( $\rho = 5.62(2) \text{ g cm}^{-3}$ ), we conclude that the  $Z$  value is 36 with one Bi atom per formula unit.

#### 2.2.3. Raman spectroscopy

Raman scattering spectra were recorded with a multi-channel Jobin-Yvon T64000 spectrophotometer connected to a CCD detector using the 514 nm excitation line. The resolution was equal to  $3 \text{ cm}^{-1}$  in the  $35\text{--}600 \text{ cm}^{-1}$  spectra range. The unknown title compound was analyzed and compared to  $[\text{Bi}_6\text{O}_4(\text{OH})_4](\text{NO}_3)_6 \cdot 4\text{H}_2\text{O}$  [5],  $[\text{Bi}_6\text{O}_5(\text{OH})_3](\text{NO}_3)_5 \cdot 3\text{H}_2\text{O}$  [4],  $[\text{Bi}_6\text{O}_{4.5}(\text{OH})_{3.5}]_2(\text{NO}_3)_{11}$  [7] and  $\text{Bi}_2\text{O}_2(\text{OH})(\text{NO}_3)$  [14] chosen as reference samples. The Raman spectra of the title compound is very similar to the  $[\text{Bi}_6\text{O}_{4.5}(\text{OH})_{3.5}]_2(\text{NO}_3)_{11}$ ,  $[\text{Bi}_6\text{O}_5(\text{OH})_3](\text{NO}_3)_5 \cdot 3\text{H}_2\text{O}$  and  $[\text{Bi}_6\text{O}_4(\text{OH})_4](\text{NO}_3)_6 \cdot 4\text{H}_2\text{O}$  spectra (Fig. 2). Four prominent vibrational modes at around 85, 105, 149 and  $180 \text{ cm}^{-1}$  can be observed in the title compound Raman spectrum. Those bands are characteristics of a model with  $[\text{Bi}_6\text{O}_x(\text{OH})_{8-x}]^{(10-x)+}$  hexanuclear entities (for instance, in  $[\text{Bi}_6\text{O}_4(\text{OH})_4](\text{ClO}_4)_6 \cdot 7\text{H}_2\text{O}$ : 92, 109, 150 and  $186 \text{ cm}^{-1}$  in the solid and 87, 104, 150 and  $178 \text{ cm}^{-1}$  in solution [15]). But at this stage, the vibrational mode positions could not be unambiguously assigned to the presence of **A** =  $[\text{Bi}_6\text{O}_5(\text{OH})_3]^{5+}$  or **B** =  $[\text{Bi}_6\text{O}_4(\text{OH})_4]^{6+}$  polycations. It is worth noticing that for  $\text{Bi}_2\text{O}_2(\text{OH})(\text{NO}_3)$ , which is built from  $\text{Bi}_2\text{O}_2^{2+}$  layers [14], the spectrum is completely different, excluding unambiguously this kind of layered structural arrangement.

#### 2.2.4. Nitrate assay

To distinguish between **A** and **B**, the conversion of the nitrate to ammonia was realized with the Devarda's alloy (50%Cu–45%Al–5%Zn) in a 1.2 N HCl solution with addition of a NaOH solution. The reaction was completed after 1 h. The ammonia was subsequently distilled and collected in a 4% boric acid solution with a Kjeldhal indicator, until a neutral pH of the condensate was obtained. The obtained solution was finally titrated by a 0.2 N HCl solution. The nitrate assay of the title compound led to the Bi/NO<sub>3</sub> ratio of 0.89. As shown by the Raman

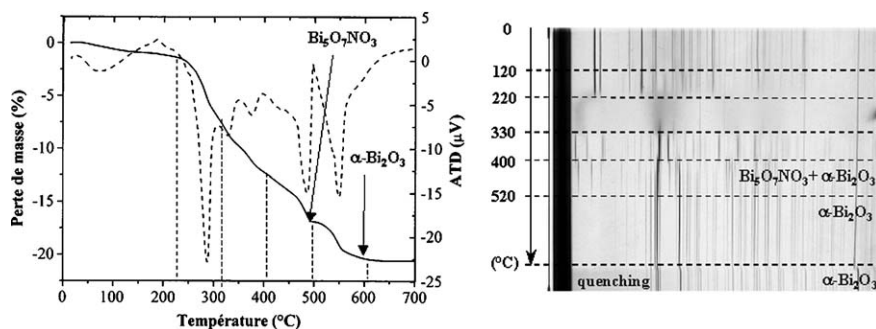


Fig. 1. (a) Thermogravimetry and differential thermal analyses of  $[\text{Bi}_6\text{O}_4(\text{OH})_4](\text{NO}_3)_6$  (b) compared to high-temperature X-ray diffraction.

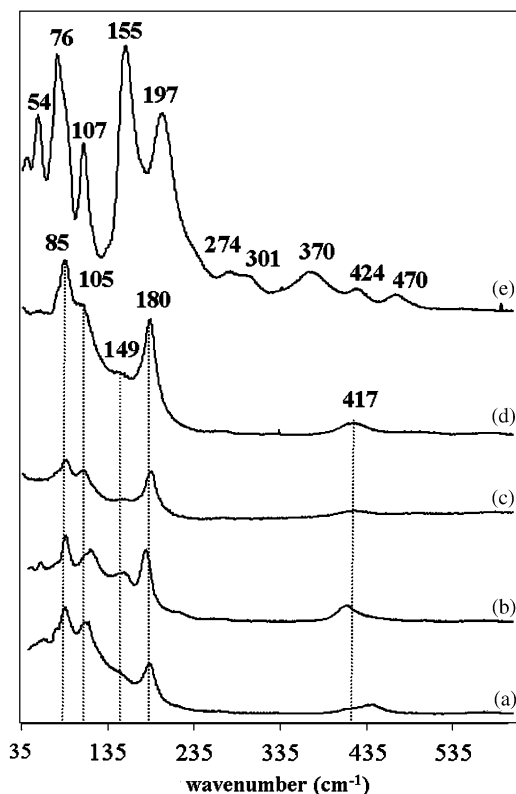


Fig. 2. Raman spectra of (a)  $[\text{Bi}_6\text{O}_4(\text{OH})_4](\text{NO}_3)_6 \cdot 4\text{H}_2\text{O}$ , (b)  $[\text{Bi}_6\text{O}_5(\text{OH})_3](\text{NO}_3)_5 \cdot 3\text{H}_2\text{O}$ , (c)  $[\text{Bi}_6\text{O}_{4.5}(\text{OH})_{3.5}]_2(\text{NO}_3)_{11}$ , (d) the title phase and (e)  $\text{Bi}_2\text{O}_2(\text{OH})(\text{NO}_3)$ .

scattering spectra, the new nitrate likely corresponds to either  $[\text{Bi}_6\text{O}_5(\text{OH})_3](\text{NO}_3)_5 \cdot x\text{H}_2\text{O}$  ( $\text{Bi}/(\text{NO}_3)^- = 1.2$ ), or  $[\text{Bi}_6\text{O}_4(\text{OH})_4](\text{NO}_3)_6 \cdot y\text{H}_2\text{O}$  ( $\text{Bi}/(\text{NO}_3)^- = 1$ ) or to the mixed  $[\text{Bi}_6\text{O}_{5-v}(\text{OH})_{3+v}](\text{NO}_3)_{5+v} \cdot z\text{H}_2\text{O}$  ( $1 < \text{Bi}/(\text{NO}_3)^- < 1.2$ ). Our results are in best agreement with the second formula, i.e.  $[\text{Bi}_6\text{O}_4(\text{OH})_4](\text{NO}_3)_6 \cdot y\text{H}_2\text{O}$ . With this information,  $y$  can be deduced from the total TGA weight loss (20.7% corresponding to 60.7 g/mole of bismuth): the weight loss during the decomposition of  $1/6[\text{Bi}_6\text{O}_4(\text{OH})_4](\text{NO}_3)_6 \cdot y\text{H}_2\text{O}$  into  $\text{Bi}_2\text{O}_3$  is equal to  $60 + 3y$ , giving  $y$  equal to 0; this strongly suggests the anhydrous formula  $[\text{Bi}_6\text{O}_4(\text{OH})_4](\text{NO}_3)_6$ . Note that this conclusion is in disagreement with the  $[\text{Bi}_6\text{O}_5(\text{OH})_3](\text{NO}_3)_5 \cdot 2\text{H}_2\text{O}$  formulation predicted by Christensen et al. [11] who deduced the formula from TGA and spectroscopic analyses only.

### 2.3. Data processing and structure determination

Unfortunately, all attempts to grow single crystals with suitable size for a structure determination on a conventional laboratory single-crystal X-ray diffractometer were unsuccessful. Indeed, even often a long exposure time, the intensities were not meaningful.

Ab initio structure determination attempts from X-ray powder diffraction using data collected with either a  $\theta$ - $2\theta$  Siemens D5000 diffractometer or an Xpert-Pro in Debye-Scherrer geometry (0.2 mm diameter capillary) have

been meaningless due to strong preferred orientation effects or strong absorption of the sample. The best results were obtained with a Huber G670 diffractometer using an asymmetric Guinier flat sample transmission geometry, equipped with a 2D detector (imaging plate),  $2\theta$  range  $6$ – $100^\circ$ ,  $\text{CuK}\alpha 1$  radiation, 2 h exposure time.

At this stage, careful examination of the extinctions deduced from the observed X-ray powder diffraction pattern ( $hkl$ :  $-h+k+l = 3n$ ) led us to propose as possible space groups  $R3$ ,  $R-3$ ,  $R32$ ,  $R3m$  and  $R-3m$ . The weak intensities of reflections with odd values of  $l$  indicate a superstructure phenomenon, later confirmed from the single crystal results. This can therefore explain the previously reported parameters ( $a = 15.57 \text{ \AA}$  and  $c = 7.6 \text{ \AA}$ ) [8–10]. The five possible space-groups were tested with the ab initio crystal structure solution software from diffraction data using direct space models, FOX [16], using the formula  $[\text{Bi}_6\text{O}_4(\text{OH})_4](\text{NO}_3)_6$  and the knowledge of a structure based on  $[\text{Bi}_6\text{O}_4(\text{OH})_4]^{6+}$  hexanuclear entities. The best fit was obtained for the space group  $R-3$ . However, the deduced positions lead to unacceptable Bi–Bi distances (1.72 Å), which can be explained by a disorder of the Bi atoms. Indeed, the Bi atoms are located at the corners of two intermixed  $\text{Bi}_6$  octahedra present in the  $[\text{Bi}_6\text{O}_x(\text{OH})_{8-x}]^{(10-x)+}$  entities, inducing a 0.5 occupancy factor. The Bi–Bi distances in each isolated  $\text{Bi}_6$  range from 3.6 to 3.8 Å, in good agreement with the average Bi–Bi distances in the reported bismuth basic nitrates [4–7]. Therefore, it is interesting to notice that each disordered  $\text{Bi}_6$  is related by a pseudo- $c/2$  translation. This phenomenon is not true for the oxygen and  $\text{NO}_3^-$  groups obtained below by microcrystal diffraction that are at the origin of the superstructure. All attempts to find a more suitable space group, in agreement with ordered Bi octahedra, failed, even with lower symmetry. After refining the Bi positions using the JANA2000 software [17], the difference Fourier series allowed us to find approximate O positions for the  $[\text{Bi}_6\text{O}_4(\text{OH})_4]^{6+}$  polycations. Note also that these O positions are disordered with some suspicious Bi–O distances (from 1.89 to 2.76 Å). At this point, we were not able to locate the  $(\text{NO}_3)^-$  groups and so further experiments were necessary.

A  $0.045 \times 0.005 \times 0.005 \text{ mm}^3$  needle-like sample was then selected and data collected using the microcrystal diffraction facility on station 9.8 [18,19] of the Synchrotron Radiation Source, CCLRC Daresbury Laboratory.

The data were collected on a Bruker Nonius APEX II CCD area-detector diffractometer [20]. The crystal was mounted at the end of a two-stage glass fiber with perfluoropolyether oil. In order to improve the diffracted intensities, the sample was cooled at 150 K by a Cryo-stream nitrogen-gas stream [21]. The wavelength was calibrated by measurement of the unit cell parameters of a standard crystal of known structure. Data collection nominally covered a sphere of reciprocal space by three series of  $\omega$ -rotation exposure frames with different crystal orientation  $\phi$  angles. Reflection intensities were integrated

using standard procedures [22], allowing for the plane-polarized nature of the primary synchrotron beam. Corrections were applied semi-empirically for absorption and incident beam decay [22]. Unit cell parameters were refined from the observed  $\omega$  angles of all strong reflections in the complete data sets. See Table 1 for additional information.

Using the  $hkl$  layer reconstruction facility of the APEX2 software, large amounts of diffuse scattering were observed. Indeed, as seen on Fig. 3 ( $hk0$  precession layer), some intense Bragg spots are superimposed on a honey-

Table 1  
Crystallographic data for  $[\text{Bi}_6\text{O}_4(\text{OH})_4](\text{NO}_3)_6$

1—Physical, crystallographic, and analytical data

Formula	$\text{Bi}_6\text{N}_6\text{O}_{26}\text{H}_4$
Crystal color	Colorless
Molecular weight ( $\text{g mol}^{-1}$ )	1757.93
Crystal system	Trigonal
Space group	$R\bar{3}$
Temperature (K)	150(2)
Cell parameters (from 3727 reflections collected on CCD)	
$a$ (Å)	15.1736(12)
$c$ (Å)	15.763(2)
$V$ (Å <sup>3</sup> )	3143.0(6)
$Z$	6
Density (calc./obs.)	5.5707/5.62(2) $\text{g cm}^{-3}$
Crystal description	Needle
Crystal size ( $\text{mm}^3$ )	$\sim 0.045 \times 0.005 \times 0.005$

2—Data collection

Diffractometer	Bruker APEX II CCD diffractometer
Monochromator	Silicon 111
Radiation type	Synchrotron
Radiation source	Daresbury SRS station
	9.8 ( $\lambda = 0.6933$ Å)
Scan mode	$\phi$ and $\omega$
No. of measured reflections	11,642
$hkl$ range	$-21 \leq h \leq 20$ $-21 \leq k \leq 21$ $-22 \leq l \leq 22$
$\theta$ range (deg)	2.02–30.51
$F(000)$	716

3—Data reduction

Linear absorption coeff. ( $\text{mm}^{-1}$ )	53.79
Absorption correction	SADABS
$T_{\text{min}}/T_{\text{max}}$	0.532
No. of independent reflections	2094
Criteria for observed reflections	$I > 3\sigma(I)$
$R_{\text{int}}$ (obs.)	6.51
Average redundancy	5.56
No. of observed reflections	1607

4—Refinement

Refinement	$F$
$R^a$ (obs./all)	0.0838/0.1008
$Rw^a$ (obs./all)	0.1272/0.1285
Data/restraints/parameters	2094/34/93
Weighting scheme	$1/\sigma^2$
Secondary extinction coeff.	None
Difference Fourier residues	$[-1.88, +2.31] \text{e}^-/\text{Å}^3$

$$^a R = \sum ||F_o| - F_c| / \sum |F_o|, Rw = [\sum w(|F_o| - |F_c|)^2 / \sum w(|F_o|^2)]^{1/2}.$$

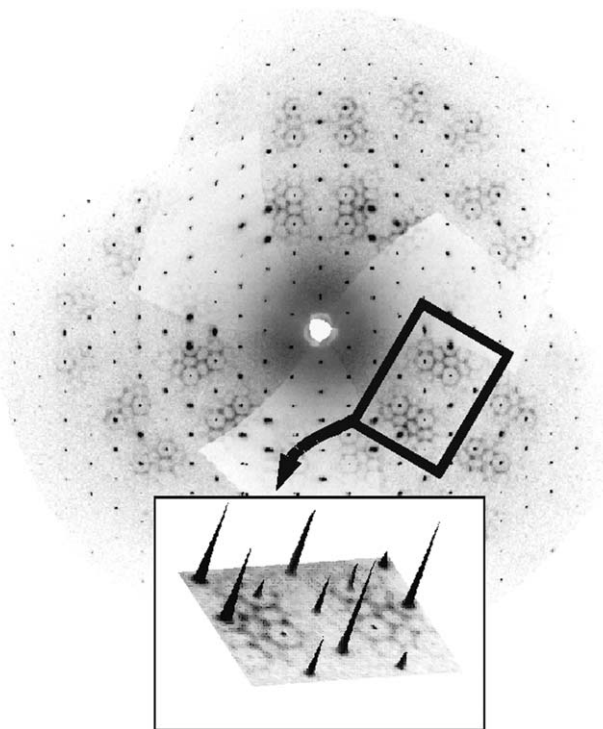


Fig. 3.  $hk0$  layer reconstruction showing some intense Bragg diffractions and a large amount of diffuse diffraction with details for the relative intensities.

comb-like diffuse scattering network. This scattering could be related to an incomplete ordering of the polycations. Although this diffuse scattering is quite important, it was not possible to take it into account in the refinement of the structural model using classical techniques. The reconstructed precession layers confirmed low intensities for layers with  $l = 2n + 1$ . As for the powder study, except for the  $R$  lattice extinctions ( $hkl: -h+k+l = 3n$ ), no extra systematic absences are observed. Surprisingly, no acceptable solution was obtained either by direct methods or by heavy atoms ones, whatever the space group ( $R3$ ,  $R\bar{3}$ ,  $R32$ ,  $R3m$  and  $R\bar{3}m$ ). Then, the single-crystal data refinement was performed with JANA2000 [17] with the Bi positions previously obtained from the powder solution. After positional and anisotropic displacement parameter refinement of Bi atoms only, the residual factor yielded  $R = 0.14$ . All the oxygen atoms of the two disordered  $[\text{Bi}_6\text{O}_4(\text{OH})_4]^{6+}$  entities were found in difference Fourier synthesis maps and introduced in the structural model taking into account the disorder (i.e. with their correct occupancy factor). The next difference Fourier synthesis residues allowed us to locate two  $[\text{NO}_3]^-$  groups. One of these groups was also disordered on two positions (hereafter labeled N4a and N4b). It is worth noticing that one oxygen atom O41 is shared by the two disordered ions. The superstructure is partially due to the two independent  $[\text{NO}_3]^-$  groups (N3 and N4) which are not related by the pseudo- $c/2$  translation, but oxygen atoms of the polycations also participate. The ratio of nitrate groups versus

bismuth by cell atoms is in complete agreement with the previous formula determination by analysis:  $[\text{Bi}_6\text{O}_4(\text{OH})_4](\text{NO}_3)_6$ . To obtain more realistic  $[\text{NO}_3]^-$  geometries, soft restraints were introduced on both the N–O distances (1.25(2) Å) and the O–N–O angles (120(1)°). At this stage, the residual factor was equal to  $R = 0.074$  with high atomic displacement parameters for the  $[\text{NO}_3]^-$  groups atoms. Soft constraints were also introduced on the isotropic displacement parameters (for each  $[\text{NO}_3]^-$  group 3 and 4, the O and N atoms being given the same isotropic atomic displacement parameter). Two relatively high positive residues on the difference Fourier synthesis maps were still observed near the O11 and O21 atoms, both 50% occupied. They were split and labeled O11/O11b and O21/O21b, respectively. The occupancy value of the O11 and O11b (O21 and O21b) deduced from the bond valence calculation and the formula, are fixed to 5/12 and 1/12, respectively (see below). Note that because of the large amount of diffuse scattering, and consequently errors on the intensities, “light” atoms are difficult to precisely locate. Finally, because of the  $[\text{Bi}_6\text{O}_4(\text{OH})_4]^{6+}$  polycations disorder and of the contrast between Bi and O atoms, we have also chosen to constrain the oxygen isotropic atomic displacement parameters to be equal. The residual factor slightly increased to  $R1 = 0.08$  (Table 1) but remains acceptable since the disorder and the diffuse were not taken into account. The introduction of a secondary extinction parameter did not improve the convergence. The presence of water molecules was ruled by the absence of extra empty space using the Platon program [23] and a hypothetical

ideal ordered structure. Attempts to locate H atoms turned out to be overoptimistic, and consequently they were not introduced in the calculation. However, their presence will be discussed later on the basis of the overall charge equilibrium and bond valence sum calculations. The final  $R$  values are then  $R = 0.0838$  and  $Rw = 0.1272$  ( $1/\sigma^2$  weighting scheme) for 1607 reflections, 34 restraints and 93 parameters. A final difference Fourier map did not reveal any peak greater than  $2.31 \text{ e}^-/\text{Å}^3$ . Positional and atomic displacement parameters are gathered in Tables 2 and 3. All attempts to find a more suitable space group, even a lower symmetry, in agreement with ordered Bi octahedra, failed. However, this paper intends to settle the question of the stoichiometry of a compound in the Bi–O– $\text{NO}_3$  system. Then the formula determination and the structural determination from microcrystals are in good agreement and yield the same anhydrous formula  $[\text{Bi}_6\text{O}_4(\text{OH})_4](\text{NO}_3)_6$ .

### 3. Structure description and discussion

#### 3.1. Assignment of the true polycations

The structure of  $[\text{Bi}_6\text{O}_4(\text{OH})_4](\text{NO}_3)_6$  is built from two disordered  $[\text{Bi}_6\text{O}_4(\text{OH})_4]^{6+}$  hexanuclear clusters called **H1** and **H2** (Fig. 4). 3Bi1a and 3Bi1b (or 3Bi2a and 3Bi2b) atoms are located at the corners of two intermixed nearly regular octahedra (Fig. 4). For each octahedron, the Bi–Bi distances range from 3.537(3) to 3.720(2) Å, in fair agreement with the mean Bi–Bi distance observed in the

Table 2

Fractional atomic coordinates, equivalent isotropic displacement parameters ( $\text{Å}^2$ , Bi), isotropic displacement parameters ( $\text{Å}^2$ , N and O), and s.u.'s for  $[\text{Bi}_6\text{O}_4(\text{OH})_4](\text{NO}_3)_6$

Atom	Wyck.	Occ.	<i>x</i>	<i>y</i>	<i>z</i>	<i>U</i> <sub>iso</sub>
Bi1a	18 <i>f</i>	0.5	0.79406(9)	0.31992(9)	0.18635(9)	0.0505(6)
Bi1b	18 <i>f</i>	0.5	0.85476(8)	0.86801(8)	0.34246(8)	0.0459(5)
Bi2a	18 <i>f</i>	0.5	0.87265(9)	0.85922(9)	0.14704(9)	0.0504(6)
Bi2b	18 <i>f</i>	0.5	0.32000(9)	0.79844(8)	0.32402(8)	0.0462(6)
O1	6 <i>c</i>	1	0	0	0.3714(7)	0.026(2)
O2	6 <i>c</i>	1	0	0	0.0820(7)	0.026(2)
O11	18 <i>f</i>	1/12	0.116(2)	0.103(2)	0.793(2)	0.026(2)
O11b	18 <i>f</i>	5/12	0.160(3)	−0.001(3)	0.175(2)	0.026(2)
O12	18 <i>f</i>	0.5	0.153(2)	0.991(2)	0.690(1)	0.026(2)
O21	18 <i>f</i>	1/12	0.117(2)	0.014(2)	0.792(2)	0.026(2)
O21b	18 <i>f</i>	5/12	0.161(3)	0.002(3)	0.825(2)	0.026(2)
O22	18 <i>f</i>	0.5	0.165(2)	0.015(2)	0.307(1)	0.026(2)
N3	18 <i>f</i>	1	0.0468(8)	0.522(2)	0.1593(7)	0.117(3)
O31	18 <i>f</i>	1	0.001(1)	0.500(2)	0.0948(9)	0.117(3)
O32	18 <i>f</i>	1	0.0009(8)	0.5007(9)	0.2288(9)	0.117(3)
O33	18 <i>f</i>	1	0.1406(1)	0.583(2)	0.1573(9)	0.117(3)
O41	18 <i>f</i>	1	0.001(2)	0.308(2)	0.001(1)	0.127(4)
N4a	18 <i>f</i>	0.5	−0.038(2)	0.231(2)	0.047(2)	0.127(4)
O42a	18 <i>f</i>	0.5	−0.037(2)	0.153(2)	0.023(2)	0.127(4)
O43a	18 <i>f</i>	0.5	−0.099(2)	0.221(2)	0.102(2)	0.127(4)
N4b	18 <i>f</i>	0.5	0.031(2)	0.265(2)	−0.045(2)	0.127(4)
O42b	18 <i>f</i>	0.5	0.010(2)	0.177(2)	−0.028(2)	0.127(4)
O43b	18 <i>f</i>	0.5	0.099(2)	0.315(2)	−0.097(2)	0.127(4)

<sup>a</sup>Constrain to be equal.

Table 3  
Anisotropic displacement parameters  $U^{ij}$  ( $\text{\AA}^2$ ) and s.u.'s for  $[\text{Bi}_6\text{O}_4(\text{OH})_4](\text{NO}_3)_6$

Atom	$U_{11}$	$U_{22}$	$U_{33}$	$U_{12}$	$U_{13}$	$U_{23}$
Bi1a	0.0379(7)	0.0467(7)	0.0712(9)	0.0243(6)	-0.0182(5)	-0.0105(5)
Bi1b	0.0349(6)	0.0397(6)	0.0519(7)	0.0103(5)	0.0121(4)	0.0022(4)
Bi2a	0.0379(7)	0.0359(6)	0.0709(9)	0.0136(5)	-0.0179(5)	-0.0075(5)
Bi2b	0.0550(7)	0.0396(6)	0.0520(7)	0.0296(5)	-0.0105(5)	0.0012(4)

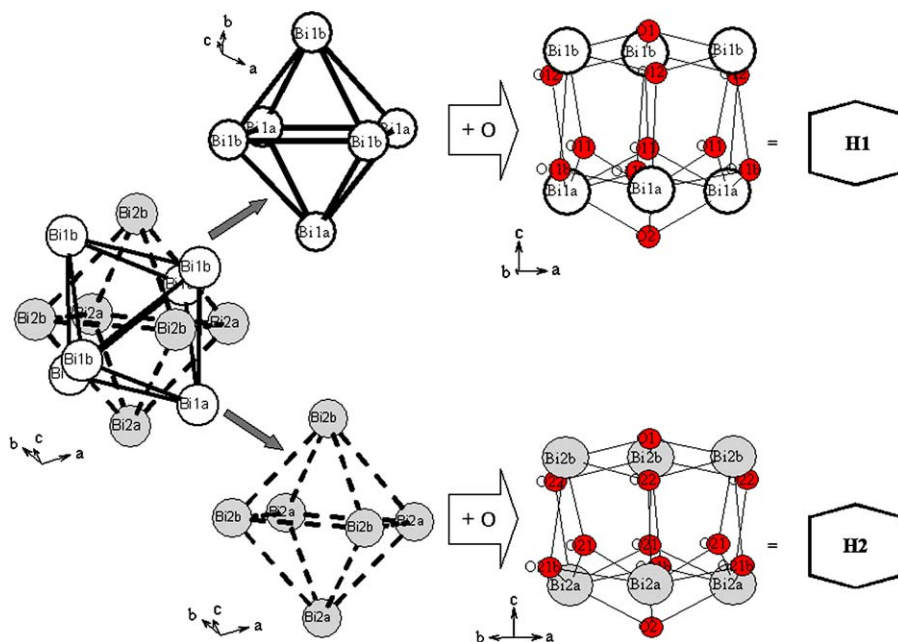


Fig. 4. Representation of the two disordered polycations  $[\text{Bi}_6\text{O}_4(\text{OH})_4]^{6+}$  in  $[\text{Bi}_6\text{O}_4(\text{OH})_4](\text{NO}_3)_6$ .

other bismuth basic nitrates [5–7]. With respect to reasonable Bi–O bond lengths, **H1** corresponds to  $[(\text{Bi}1\text{a}, \text{Bi}1\text{b})_6 \text{O}12_3(\text{O}11, \text{O}11\text{b})_3]$  while **H2** corresponds to  $[(\text{Bi}2\text{a}, \text{Bi}2\text{b})_6 \text{O}22_3(\text{O}21, \text{O}21\text{b})_3]$ . The O atoms cap the faces of the bismuth, defining  $[\text{O}Bi_3]$  triangular-based pyramids.

### 3.2. $\text{O}^{2-}$ versus $\text{OH}^-$

As already pointed out for  $[\text{Bi}_6\text{O}_{4.5}(\text{OH})_{3.5}]_2(\text{NO}_3)_{11}$  [7], the oxygen bond-valence parameter calculation can lead to discrimination between the oxo oxygen atoms and the hydroxyl oxygen atoms of the hexanuclear polycation. For the two  $[\text{Bi}_6\text{O}_4(\text{OH})_4]^{6+}$  disordered polycations of the title compound, the bond valence sum calculations discriminate between three types of oxygen atoms using Brown and Altermatt data [24] ( $r_0 = 2.094$  and  $B = 0.37$ ) (Table 4):

- $v$  of ca. 1.4 can be attributed to hydroxyl oxygen atoms (i.e. O11b, O12, O21b and O22);
- bond valence parameters of ca. 2.6 (i.e. O1, O11 and O21) can be assigned to oxo oxygen atoms;
- intermediate  $v$  value (ca. 1.8), found in the two polycations, corresponds to the O2 sites, which are populated by 50% oxo oxygen atoms and 50% hydroxyl oxygen atoms.

Let us call  $x/2$  the O*i*1 occupancy ( $i = 1$  for cluster **H1** and  $i = 2$  for **H2**). The discrimination between the oxo oxygen atoms and the hydroxyl oxygen atoms yields to the formula  $[\text{Bi}_6(\text{O}1)(\text{O}2)_{0.5}(\text{O}i1)_x(\text{O}i2\text{H})_3(\text{O}i1\text{bH})_{3-x}]^{6+}$ . Then, to obtain the O/OH ratio, in agreement with the  $[\text{Bi}_6\text{O}_4(\text{OH})_4](\text{NO}_3)_6$  formula determined by analysis and microcrystals diffraction,  $x$  must be equal to 2.5. So, the occupancy of the O11 and O11b (O21 and O21b) atoms are 5/12 and 1/12, respectively. Note that 1/12 of one oxygen atom represents only 2/3 of an electron, which is not possible to refine from an X-ray diffraction experiment but this oxygen split is necessary to obtain compound neutrality and has thus been fixed.

### 3.3. Polycationic ordering

The  $[\text{Bi}_6\text{O}_4(\text{OH})_4]^{6+}$  hexanuclear clusters form columns running down the  $c$ -axis with respect to a local ordering between **H1** and **H2** mainly induced by hydrogen bonds and O–O repulsion. As shown in Fig. 5, between successive polycations, pairs of oxygen atoms point toward each other and alternate along the  $c$ -axis: O1/O1 ( $d = 4.05(2)$  Å) and O2/O2 ( $d = 2.58(2)$  Å). The latter distance (50% oxo oxygen atoms and 50% hydroxyl oxygen atoms) appears perfectly suitable for an O–H–O hydrogen bonding scheme

Table 4  
Distances (Å) and Valence Bond Sum Parameters for the oxygen atoms of the hexanuclear clusters  $[\text{Bi}_6\text{O}_4(\text{OH})_4](\text{NO}_3)_6$

Polycation 1					Polycation 2				
$O_i$	$\text{Bi}_j$	$d(\text{O}_i\text{--Bi}_j)$	$v_i$	$v$	$O_i$	$\text{Bi}_j$	$d(\text{O}_i\text{--Bi}_j)$	$v_i$	$v$
O1	Bi1b	2.159(2)	0.839	<b>2.52 → O</b>	O1	Bi2b	2.156(3)	0.846	<b>2.54 → O</b>
	Bi1b	2.159(2)	0.839			Bi2b	2.156(3)	0.846	
	Bi1b	2.159(2)	0.839			Bi2b	2.156(3)	0.846	
O2	Bi1a	2.285(5)	0.597	<b>1.79 → O/OH</b>	O2	Bi2a	2.285(5)	0.597	<b>1.79 → O/OH</b>
	Bi1a	2.285(5)	0.597			Bi2a	2.285(5)	0.597	
	Bi1a	2.285(5)	0.597			Bi2a	2.285(5)	0.597	
O11	Bi1a	2.09(3)	1.011	<b>2.69 → O</b>	O21	Bi2a	2.09(3)	1.011	<b>2.71 → O</b>
	Bi1a	2.14(3)	0.883			Bi2a	2.15(2)	0.860	
	Bi1b	2.18(3)	0.793			Bi2b	2.16(3)	0.837	
O11b	Bi1a	2.15(5)	0.860	<b>1.45 → OH</b>	O21b	Bi2a	2.16(3)	0.837	<b>1.44 → OH</b>
	Bi1a	2.45(3)	0.382			Bi2a	2.44(3)	0.393	
	Bi1b	2.67(3)	0.211			Bi2b	2.67(3)	0.211	
O12	Bi1b	2.225(2)	0.702	<b>1.42 → OH</b>	O22	Bi2b	2.34(2)	0.514	<b>1.32 → OH</b>
	Bi1b	2.38(2)	0.459			Bi2b	2.33(2)	0.521	
	Bi1b	2.59(2)	0.258			Bi2b	2.55(2)	0.289	

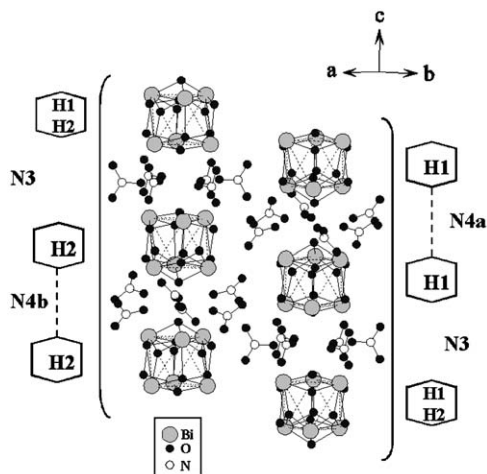


Fig. 5. Representation of the  $[\text{Bi}_6\text{O}_4(\text{OH})_4]^{6+}$  hexanuclear polycation column of the  $[\text{Bi}_6\text{O}_4(\text{OH})_4](\text{NO}_3)_6$  structure with the constrain pair H1–H1 or H2–H2.

in agreement with the previous bond-valence parameter results, so yielding a short space between the two  $[\text{Bi}_6\text{O}_4(\text{OH})_4]^{6+}$  polycations. It leads to the disorder between the  $[\text{NO}_3]^-$  group N4a and N4b (Fig. 6). The distances and angles of the nitrate groups are presented in Table 5. The oxygen atoms of N4a (O42a and O43a) are too close to Bi2a atoms (around 1.9 Å) but have acceptable distances with Bi1a atoms ( $>2.8$  Å). This implies that  $\text{N4aO}_3^-$  are located between two H1 polycations linked by a O2–H–O2 hydrogen bond. In the same manner,  $\text{N4bO}_3^-$  occupies the interstices between two H2 linked by a O2–H–O2 bond. The O1–O1 (oxo oxygen atoms) distances (4.05(2) Å) are too long to assure the cohesion of the polycations in the column. The  $[\text{N3O}_3]^-$  groups are located

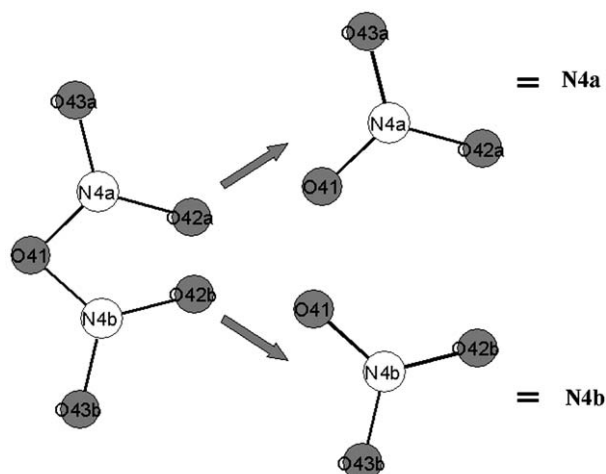


Fig. 6. Representation of the two disordered  $[\text{NO}_3]^-$  groups denoted N4a and N4b with O41 oxygen atom common to the two disordered ions.

Table 5  
Distances (Å) and angles (°) for the nitrate groups of  $[\text{Bi}_6\text{O}_4(\text{OH})_4](\text{NO}_3)_6$

$\text{N}_x$	$\text{O}_{xy}$	Distances	$\text{O}_{xy}\text{--N}_x\text{--O}_{xy}$	Angles
N3	O31	1.19(2)	O31–N3–O32	120(2)
	O32	1.25(2)	O31–N3–O33	119(2)
	O33	1.25(2)	O32–N3–O33	119(2)
N4a	O41	1.25(3)	O41–N4a–O42a	120(2)
	O42a	1.25(4)	O41–N4a–O43a	119(3)
	O43a	1.22(4)	O42a–N4a–O43a	118(2)
N4b	O41	1.21(3)	O41–N4b–O42b	119(2)
	O42b	1.24(4)	O41–N4b–O43b	120(2)
	O43b	1.24(3)	O42b–N4b–O43b	119(3)

between the polycations in an ordered manner. It is noteworthy that their oxygen corners have reasonable bonds with both Bi1b (H1) and Bi2b (H2), making a likely place for antiphase boundaries (H1–H1, H1–H2 or H2–H2) in a disordered manner. The columns are linked to each other through O–H–O hydrogen and Bi–O–N bonding schemes.

The  $[\text{Bi}_6\text{O}_4(\text{OH})_4](\text{NO}_3)_6$  density ( $5.571 \text{ g cm}^{-3}$ ) is the highest of the polycationic-bismuth-based nitrates:  $[\text{Bi}_6\text{O}_4(\text{OH})_4](\text{NO}_3)_6 \cdot \text{H}_2\text{O}$  ( $5.405 \text{ g cm}^{-3}$ ) [6] and  $[\text{Bi}_6\text{O}_4(\text{OH})_4](\text{NO}_3)_6 \cdot 4\text{H}_2\text{O}$  ( $4.973 \text{ g cm}^{-3}$ ) [5]. It can be explained by shorter distances between the polycations and the  $[\text{NO}_3]^-$  groups due to the absence of water molecules and subsequently to a greater degree of ionic cohesion.

#### 4. Conclusion

The complementary current study using powder XRD; TGA and nitrate assay for formula determination, and finally microcrystal diffraction at 150(2) K for the crystal structure refinement, ascribe the  $[\text{Bi}_6\text{O}_4(\text{OH})_4](\text{NO}_3)_6$  formula and  $a = 15.1332(6) \text{ \AA}$  and  $c = 15.7909(9) \text{ \AA}$  parameters, so refuting previous investigations. Its structure is highly disordered and shows, in general, high displacement parameters related to the high level of diffuse scattering due to local ordering only. However, the detailed analyses of bond distances and valence bond sums enable the establishment of well-ordered fragments of the structure and the most probable sites where the disorder occurs. We think that we have probably got as far as possible without modeling the diffuse scattering as well.

#### Acknowledgment

We acknowledge the provision of time on the Small Molecule Crystallography Service at the CCLRC Daresbury Laboratory via support by the European Community—Research Infrastructure Action under the FP6 “Structuring the European Research Area” Programme (through the Integrated Infrastructure Initiative “Integrat-

ing Activity on Synchrotron and Free Electron Laser Science”). We also acknowledge the help of Dr. Simon Teat in the preparation of precession images to illustrate the diffuse scattering.

#### References

- [1] P. Pascal, *Nouveau Traité de Chimie Minérale*, vol. 9, Masson, Paris, 1958, p. 795.
- [2] A.F. Holleman, E. Wiberg, *Lehrbuch der Anorganischen Chemie*, Walter de Gruyter & Co., Berlin, 1971, p. 440.
- [3] N. Henry, O. Mentre, J.C. Boivin, F. Abraham, *Chem. Mater* 13 (2001) 543.
- [4] F. Lazarini, *Acta Crystallogr. Sect. B* 34 (1978) 3169.
- [5] F. Lazarini, *Cryst. Struct. Commun.* 8 (1979) 69.
- [6] F. Lazarini, *Acta Crystallogr. Sect. B* 35 (1979) 448.
- [7] N. Henry, M. Evain, P. Deniard, S. Jobic, O. Mentré, F. Abraham, *J. Solid State Chem.* 176 (1) (2003) 127.
- [8] J. Ozols, *Latv. PSR Zinat. Akad. Vestis* 4 (1950) 87.
- [9] J. Ozols, *Latv. PSR Zinat. Akad. Vestis* 5 (1950) 83.
- [10] J. Ozols, *Latv. PSR Zinat. Akad. Vestis* 6 (1950) 49.
- [11] A.N. Christensen, M.A. Chevalier, J. Skibsted, B.B. Iversen, *J. Chem. Soc. Dalton Trans.* 3 (2000) 2265.
- [12] P.-E. Werner, L. Eriksson, M. Westdahl, *J. Appl. Crystallogr.* 18 (1985) 367.
- [13] H. Kodama, *J. Solid State Chem.* 112 (1994) 27.
- [14] N. Henry, M. Evain, P. Deniard, S. Jobic, F. Abraham, O. Mentré, *Z. Naturforsch.* 60b (2005) 322.
- [15] B. Sundvall, *Inorg. Chem.* 22 (1983) 1906.
- [16] V. Favre-Nicolin, R. Cerny, FOX Software, Free Objects for Xtal Structures, version 1.6.0.2.
- [17] V. Petricek, M. Dusek, L. Polatinus, JANA2000, A Crystallographic Computing System, Institute of Physics, Academy of Sciences of the Czech Republic, Prague, 2005.
- [18] R.J. Cernik, W. Clegg, C.R.A. Catlow, G. Bushnell-Wye, J.V. Flaherty, G.N. Greaves, I. Burrows, D.J. Taylor, S.J. Teat, M. Hamichi, *J. Synchrotron Rad.* 4 (1997) 279.
- [19] W. Clegg, M.R.J. Elsegood, S.J. Teat, C. Redshaw, V.C. Gibson, *J. Chem. Soc. Dalton Trans.* (1998) 3037.
- [20] APEX 2, Bruker Nonius, 1998.
- [21] J. Cosier, A.M. Glazer, *J. Appl. Crystallogr.* 19 (1986) 105.
- [22] SAINT version 7.06a, Bruker AXS Inc., Madison, WI, USA, 2004.
- [23] A.L. Spek, PLATON, A Multipurpose Crystallographic Tool, Utrecht University, Utrecht, The Netherlands, 2002.
- [24] I.D. Brown, D. Attermatt, *Acta Crystallogr. Sect. B* 41 (1985) 244.